A practical approach for finite-element modeling of transfer length in pretensioned, prestressed concrete members using end-slip methodology

J. Chris Carroll, Thomas E. Cousins, and Carin L. Roberts-Wollmann

- This paper presents a numerical modeling approach that accounts for slip between prestressing strands and the surrounding concrete within the transfer zone and accurately predicts member behavior based on specified transfer lengths.
- The modeling approach uses a matrix of solid elements to represent the concrete truss elements for the prestressing strand and nonlinear springs for the interface between prestressing strand and concrete.
- Comparison with experimental data confirms the practicality and accuracy of the model in predicting member behavior based on specified transfer lengths.

The analysis and design of pretensioned, prestressed concrete members is becoming more complex with advances in material technology. In many cases, advanced forms of analyses are required, such as strut-and-tie models and numerical models, especially to predict member behavior in the end zone. Unfortunately, the computational costs associated with these advanced methods can quickly escalate. There is a need for a practical approach to accurately simulate the behavior of pretensioned, prestressed concrete members, including the effects of prestress transfer. This paper presents a modeling approach that accounts for slip between prestressing strand and the surrounding concrete based on the known relationship between end slip and transfer length. The objective of the study is to develop a modeling approach that can accurately and efficiently predict member behavior, including end slip, strand force development, and concrete strains and stresses based on a specified transfer length. Twenty-three numerical models were constructed, analyzed, and compared with experimental data.

Background

Pretensioned, prestressed concrete members rely on precompression applied through internal bonded strands, which are tensioned before casting. The tensile force is transferred from the prestressing strand to the surrounding

concrete by adhesion and mechanical interlock between the two materials. Within the transfer zone, adhesion is lost during transfer due to strand slip.[1] Transfer of prestress from the prestressing strands to the surrounding concrete is achieved through mechanical interlock between the strands and the concrete and the additional friction produced due to lateral expansion of the strands at release.

Prestressing strands elongate in the direction of the applied load during tensioning, causing a reduction in the cross-sectional area due to the Poisson effect. The concrete is then placed in the formwork. When the strands are released, the now-hardened concrete restrains them from returning to their original length and cross section. As the strands retract, adhesion between the prestressing strands and surrounding concrete is broken. The strand tries to expand laterally, giving rise to circumferential stresses along its length. Mechanical interlock and friction due to the Hoyer effect[1] generate bond stresses between the strand and the surrounding concrete. The distance required to transfer the force in the prestressing strand to the surrounding concrete is the transfer length, defined by the American Concrete Institute's (ACI's) *Building Code Requirements for Structural Concrete (ACI 318-11) and Commentary (ACI 318R-11)*[2] as the distance over which the strand should be bonded to the concrete to develop the effective prestress in the prestressing steel. The effective prestress is assumed to vary linearly from zero at the end of the member to full development at the transfer length, where the strand ceases to slip and adhesion again contributes to the bond between the two materials.

ACI 318-11 and the American Association of State Highway and Transportation Officials (AASHTO) have similar criteria for calculating transfer length. In equations for the development length of prestressing strands, the first component accounts for the transfer length, while the second accounts for the flexural bond length. Equation (1) shows the expression for transfer length l_t used in the determination of development lengths for both ACI 318-11 and *AASHTO LRFD Bridge Design Specifications*,[3] which was derived based on research performed in the late 1950s and early 1960s. Janney[1] first concluded that the stress along a concrete prism was directly proportional to the tensile stresses in the pretensioned wire, though there was no strain compatibility within the transfer zone as a result of slip. Hanson and Kaar[4] later found the average bond stress to be 400 psi (2.75 MPa), based on average transfer length measurements for $^1/_4$ in. (6 mm), $^3/_8$ in. (10 mm), and $^1/_2$ in. (13 mm) diameter strands pretensioned to 150 ksi (1030 MPa). Based on an average bond stress of 400 psi, Eq. (2) was derived to estimate transfer lengths for 250 ksi (1720 MPa) stress-relieved strand. Subsequently, Janney[5] found no significant increase in transfer length, regardless of a 26% higher jacking stress using 270 ksi (1860 MPa) strand. Thus Eq. (2) was simplified to Eq. (1)[6] and was first implemented in the 1963 ACI *Building Code Requirements for Reinforced Concrete*.[7] In the shear provisions of both codes, a value of 150 ksi is assumed for the effective stress in strands after all losses f_{se}, reducing Eq. (1) to $50d_b$, where d_b is the strand diameter.

This assumption provides designers with a simplified method for obtaining the force in the strand at any distance within the transfer zone and has generally been considered conservative but was increased by AASHTO LRFD specifications to $60d_b$ to account for the higher jacking stresses typically used in industry.[8]

$$l_t = \left(\frac{f_{se}}{3}\right) d_b \qquad \text{Eq. (1)}$$

$$l_t = \left(\frac{f_{se}}{2.94}\right) d_b \qquad \text{Eq. (2)}$$

In addition to the code provisions, a number of transfer length equations have been proposed over the course of the past 60 years,[8–22] taking into consideration the stress in the strand, strand diameter, concrete strength, method of release, and vertical location of the strand. For the most part, transfer length studies have relied on measurements of concrete surface strains, which can be cumbersome and time-consuming. Although mechanical bond does resist the tendency of the strand to slip, some slip, which has been shown to be directly proportional to transfer length, occurs within the transfer length. **Figure 1** shows the theoretical relationship of the strain in the concrete and steel with respect to the distance from the end of the member.

An alternative method for measuring transfer lengths is to measure the slip between the end of the strand and the end

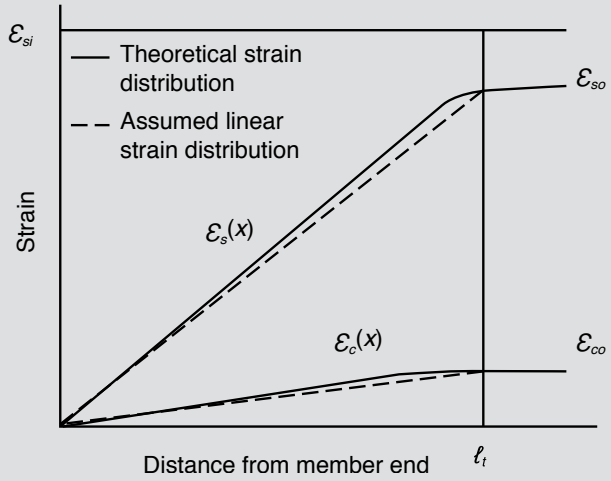

Figure 1. Concrete and steel strain distribution within transfer zone. Note: l_t = transfer length; $\varepsilon_c(x)$ = strain in concrete along transfer length; ε_{co} = strain in concrete just after transfer; $\varepsilon_s(x)$ = strain in strand along transfer length; ε_{si} = strain in strand just before transfer; ε_{so} = strain in strand just after transfer.

of the member. Assuming a linear distribution of strains (Fig. 1), the elastic shortening occurring from the end of the specimen to the end of the transfer length in the specimen itself equals the area under the curve for the strain in the concrete along the transfer length $\varepsilon_c(x)$ calculated by Eq. (3), while the shortening of the strand equals the area between the curve for the strain in the strand along the transfer length $\varepsilon_s(x)$ and the initial steel-strain plateau calculated by Eq. (4). The end slip L_{es} is equal to the difference between the shortening of the strand within the transfer zone (sum of elastic shortening and end slip) δ_s and the elastic shortening of concrete within the transfer zone δ_c (Eq. [5]) as derived by Cousins et al.[23] based on the assumption of linear variations for both concrete and steel strains. By substituting the sum of ε_{so} and ε_{co} (where ε_{co} is the strain in the concrete just after transfer, and ε_{so} is the strain in the strand just after transfer) for the strain in the strand just before transfer ε_{si} along with the stress in the strand just after transfer f_{so} and modulus of elasticity of the strand E_{ps} for the steel strain ε_{so} into Eq. (5), the transfer length can be solved by Eq. (6).

$$\delta_c = \int_0^{l_t} \varepsilon_c(x)\,dx = \frac{\varepsilon_{co} l_t}{2} \qquad \text{Eq. (3)}$$

$$\delta_s = \varepsilon_{si} l_t - \int_0^{l_t} \varepsilon_s(x)\,dx = \varepsilon_{si} l_t - \frac{\varepsilon_{so} l_t}{2} \qquad \text{Eq. (4)}$$

$$L_{es} = \varepsilon_{si} l_t - \frac{\varepsilon_{so} l_t}{2} - \frac{\varepsilon_{co} l_t}{2} \qquad \text{Eq. (5)}$$

$$l_t = \frac{2 L_{es} E_{ps}}{f_{so} + E_{ps} \varepsilon_{co}} \qquad \text{Eq. (6)}$$

Guyon[24] derived Eq. (7), accounting for the possibility of a constant bond stress distribution (linear strain distribution) or a linear bond stress distribution (parabolic strain distribution), to calculate end slip. Equation (7) includes a factor α that varies with bond stress distribution. With a constant bond stress distribution, α equals 2 and the calculated transfer length will equal that calculated by Eq. (6). However, a linear bond stress distribution results in α equal to 3. Studies by Martí-Vargas[25] and Balazs[26] found α to be 2.44 and $2/(1 - b)$, respectively, where b is the power of the bond stress relationship.

$$l_t = \alpha \frac{L_{es}}{\varepsilon_{si}} \qquad \text{Eq. (7)}$$

Transfer length is an important aspect of pretensioned, prestressed concrete, especially with respect to shear design and serviceability requirements within end-zone regions at transfer. Both ACI 318-11 and AASHTO LRFD specifications include provisions for shear design but give less guidance for end-zone analysis. Service stress limits are provided for the ends and other locations throughout a member, but the method of analysis is determined by the complexity of the end zone. In most cases, simple bending stress calculations are sufficient; in others, more advanced techniques such as strut-and-tie models, neural networks, and even numerical models may be required. Neural networks, for example, can provide accurate results but can be complex.[27–29] Likewise, numerical modeling can also provide accurate results but can be somewhat cumbersome, and the complexity can increase almost exponentially with the slightest modifications.

In many cases, numerical models of pretensioned, prestressed concrete members neglect the effects of slip within the transfer length. Two common approaches apply the prestressing force throughout the entire member length.[30] The first method considers equivalent loads applied externally to the member, while the second uses steel segments perfectly bonded to the member combined with the application of initial strains. While these approaches may be sufficient in some applications, they fail to account for slip between the concrete and prestressing strands, a relationship sometimes needing consideration for model accuracy. Kannel et al.[31] used numerical models to simulate the effects of unreleased strands on girders during transfer. The numerical models in the study used solid elements to represent the concrete and truss elements to represent the prestressing strands and applied the prestressing force using two methods: a ramped area and approximate rigid-plastic springs, both accounting for the transfer length. Ayoub and Filippou[32] and Arab et al.[33] also used numerical models to predict the behavior of pretensioned, prestressed concrete members accounting for transfer length. Ayoub and Filippou used a combination of beam-column, tendon, and bond elements to represent the behavior of the concrete, prestressing steel, and transfer of forces, respectively. The modeling technique used an initial strain applied to the tendon element to simulate the prestressing force, while the bond elements were based on the bond stress-slip relationship by Eligehausen et al.[34] for anchored reinforcing bars. Like Kannel et al., Arab et al. used solid elements to represent the concrete. The transfer of the prestressing force was simulated using two methods: an extrusion technique or friction-based model and an embedment technique using strain compatibility, both also accounting for transfer length. Each of the three studies accounting for transfer length compares well with experimental results.

As designs continue to incorporate stronger, more advanced materials, more advanced analytical methods are becoming necessary. However, the associated costs and complexity cannot outweigh the benefits of such methods. Numerical analysis of pretensioned, prestressed concrete members can accurately predict their behavior, but the

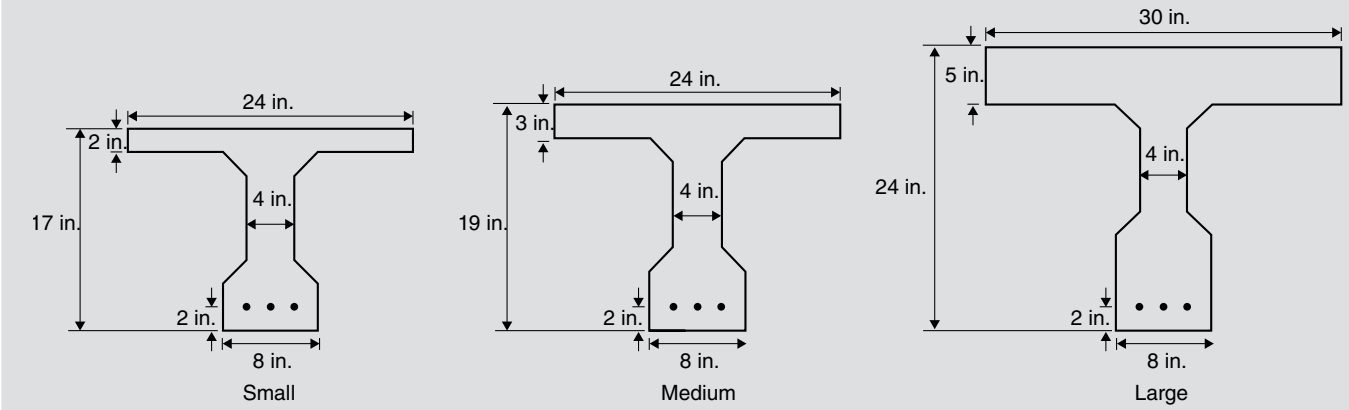

Figure 2. T beam cross sections. Note: 1 in. = 25.4 mm.

smallest of changes can increase the cost and complexity exponentially. Advanced methods of analysis are needed to predict the behavior of pretensioned, prestressed concrete members accounting for bond slip; more important, a practical method of advanced analysis is needed.

Test specimens

This study includes data from two types of test specimens: T beams and top-strand blocks (**Fig. 2** and **3**), respectively. The T beams were 24 ft (7.3 m) long and had three different cross sections corresponding to the size of prestressing strand used. The small, medium, and large beams each contained $^1/_2$ in. (13 mm) diameter regular, $^1/_2$ in. diameter super, and 0.6 in. (15 mm) diameter strands, respectively. In each cross section, three strands were placed 2 in. (50 mm) from the bottom of the formwork with a lateral center-to-center spacing of 2 in. The size and shape of the cross section were also influenced by the desired tensile strain in the strand anticipated to occur at the ultimate flexural capacity of the member. Tests have shown the development length of prestressing strands to be dependent on the strain in the strand at the time of failure. Thus as recommended by Buckner,[8] the cross sections were designed such that the strain at ultimate flexural capacity would exceed the minimum required elongation of 3.5%. Taking into consideration the strand size and desired flexural behavior at failure, the T beam test specimens used are considered to be representative of other shapes and sizes of pretensioned, prestressed concrete beams.

The top-strand block test specimens were 12 ft (3.66 m) long and also had three different cross sections, which were used to evaluate the effect of vertical position on transfer length. While $^1/_2$ in. (13 mm) diameter regular and $^1/_2$ in. diameter super strands were both used in various groups of the top-strand blocks, each individual set of blocks cast always included the same size strand in the

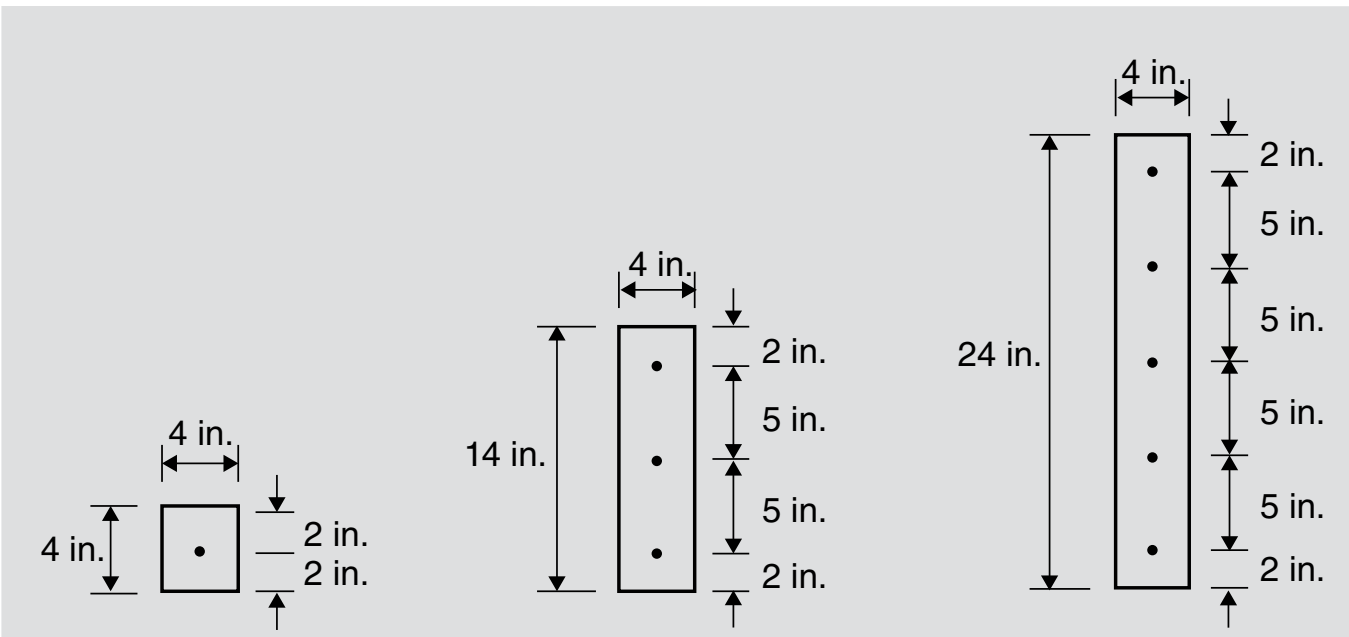

Figure 3. Top-strand blocks. Note: 1 in. = 25.4 mm.

three cross sections. The sizes of the blocks were selected based on the desired comparisons for strand vertical location but were selected with surface strain magnitudes taken into consideration. While six different cross sections were used to obtain the transfer length and end-slip data, only the small and medium T beams and the 4 × 4 in. (100 × 100 mm) prism were modeled and used for the comparisons between numerical models and experimental results presented in this paper.

End-slip reliability

A total of 119 transfer lengths were calculated based on concrete surface strains, while 57 of the 119 were also estimated using end-slip measurements. Concrete surface strains are typically measured using a demountable mechanical (DEMEC) strain gauge and surface-mounted gauge points. The DEMEC gauge has a gauge length of 8 in. (200 mm), and the gauge points are approximately $^1/_4$ in. (6 mm) in diameter with a small, fine point indention in the center. The points were placed on the test specimens at the elevation of the strands at spacings of 2 in. (50 mm) and 4 in. (100 mm) and attached using a five-minute epoxy. A spacing of 2 in. was used in areas expected to be within the anticipated transfer zone, ensuring a defined ascending branch of the strain plot, while the remaining points located beyond the anticipated transfer zone, corresponding to the strain plateau, were spaced at 4 in. Before transfer, initial measurements were obtained by taking the average of three successive measurements. Immediately after transfer, the gauge points were measured once more. The difference between the two readings at any one location provides the change in length from the point at which zero prestress force is applied to the point at which the entire prestress force is applied. The change in length is then divided by the gauge length, resulting in the average strain across the gauge length for that location. Based on each set of concrete surface strains, strain profiles were created for each transfer zone and the 95% average maximum strain method was used to estimate the transfer lengths.[35]

The end-slip measurements were taken at the dead end of the test specimens using a depth micrometer and U brackets attached directly to the strands. The U brackets were placed approximately 1 in. (25 mm) from the face of the test specimen on each strand with a hose clamp providing a stationary reference point for measurements before and after transfer. Measurements were not taken at the live end of the test specimens as a result of the U brackets bending and hose clamps breaking during transfer. A small aluminum flat bar was also embedded in the concrete during casting to provide a smooth, flat surface for measuring. As with the DEMEC points, three initial measurements were taken before transfer and were averaged to ensure an accurate reference point. Following transfer, measurements were again taken with the end slip equal to the distance between the initial and final measurements minus the elastic shortening of the protruding strand. There is an approximately linear relationship between the transfer lengths calculated from concrete surface strains and their corresponding end slips (**Fig. 4**). Furthermore, transfer lengths were calculated from end-slip measurements using Eq. (6) and compared with the transfer lengths calculated from concrete surface strains. **Figure 5** shows the relationship of transfer lengths calculated using concrete surface strains with respect to transfer lengths calculated using Eq. (6), showing a good correlation. Eq. (6) was used for the development of the numerical models in this study because of its theoretical accuracy.

Numerical modeling approach

The analytical models presented in this study are constructed using GT STRUDL structural design and analysis software. More complex finite element packages have existing contact elements, but the goal of this modeling approach is to limit model complexity. Each model comprises three components:

- a matrix of solid brick elements representing the concrete
- truss elements representing the prestressing strands
- nonlinear spring elements accounting for the interface between the prestressing strands and the surrounding concrete

Both the solid elements and truss elements use a linear elastic material and are assumed to remain elastic. The nonlinear springs have a bilinear force-versus-displacement relationship and are used to account for the slip between strand and concrete. The solid elements and truss elements are not directly connected. Instead, a series of duplicate joints is generated along the line corresponding to the desired location of the prestressing strand(s), to which the truss elements are attached. Joint constraints are applied to the duplicate joints, restraining their movement in all directions to that of their counterpart except in the direction of the truss elements. In the direction of the truss elements, the movement of the duplicate joints relative to their counterpart is controlled by the nonlinear spring elements. Contrary to the modeling techniques used in other studies, the force-versus-displacement curves for the nonlinear spring elements are based solely on the relationship between end slip and transfer length.

The effective prestress is assumed to vary linearly from zero at the end of the member to full development at the transfer length, where the strand ceases to slip. However, the transfer length would be better represented by two regions[24] (**Fig. 6**), a plastic zone and a much shorter elastic zone as defined by Cousins et al.[11] Within the plastic zone, the stress in the strand increases with a linear variation.

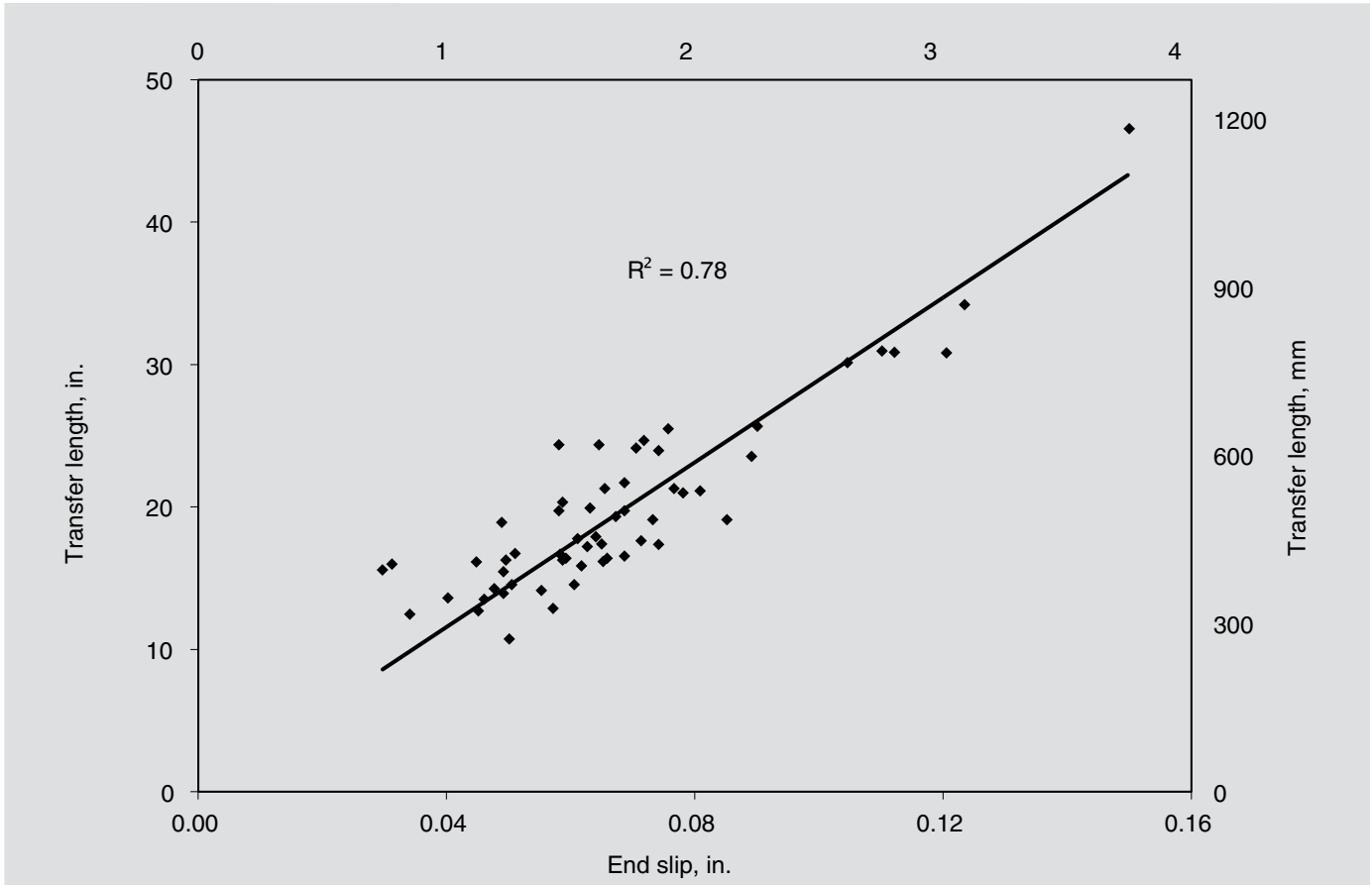

Figure 4. Correlation of transfer lengths from concrete surface strains with end-slip measurements. Note: R^2 = coefficient of determination.

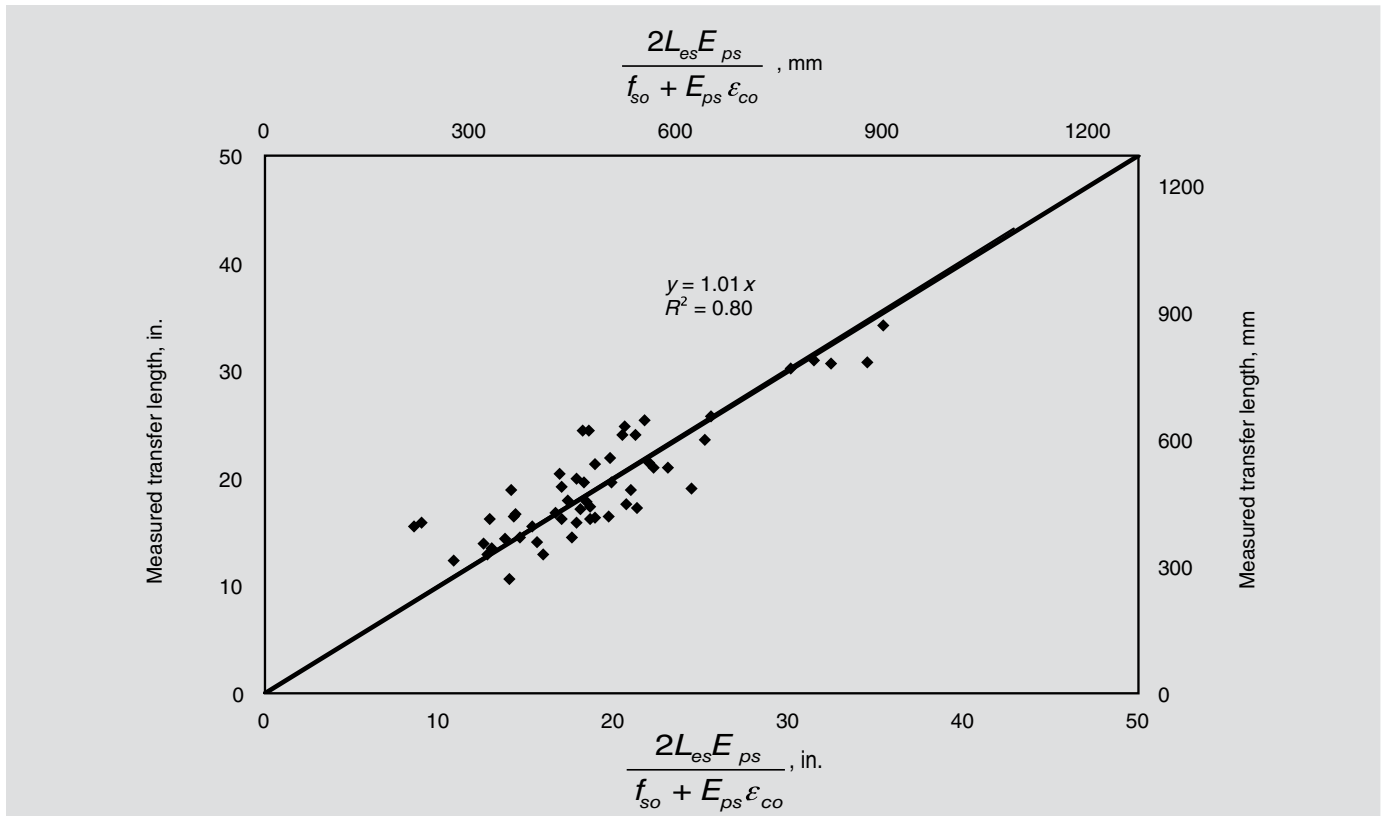

Figure 5. Correlation of transfer lengths from concrete surface strains with transfer lengths calculated using Eq. (6). Note: E_{ps} = modulus of elasticity of prestressing strands; f_{so} = stress in strand just after transfer; L_{es} = end slip; R^2 = coefficient of determination; ε_{co} = strain in concrete just after transfer.

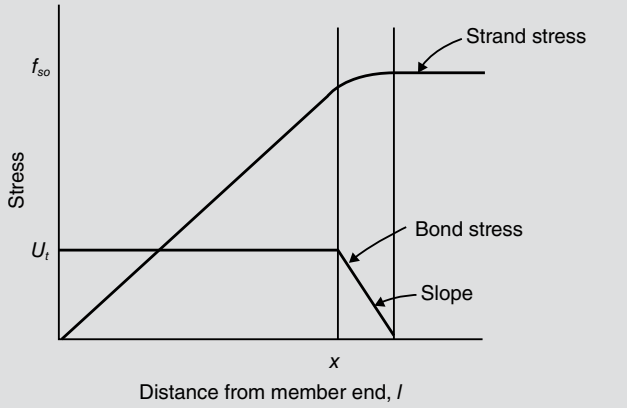

Figure 6. Assumed bond stress and strand stress distribution within transfer zone. Note: f_{so} = stress in strand just after transfer; U_t = plastic transfer bond stress; x = distance from end of member.

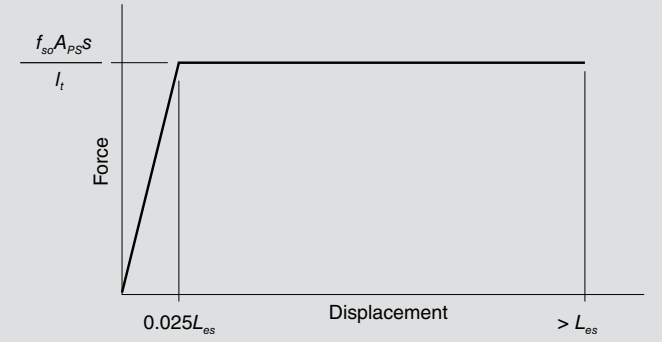

Figure 7. Nonlinear spring force–versus–displacement curve. Note: A_{ps} = area of prestressing strand; f_{so} = stress in strand just after transfer; l_t = transfer length; L_{es} = end slip; s = nonlinear spring spacing.

Within this region, a gradual buildup of force occurs along the interface between the prestressing strand and the surrounding concrete, creating a constant bond stress. Before the force in the strand reaches its maximum, the increase in strand stress must gradually decrease to zero, likewise the bond stress, occurring within the elastic zone.

As previously discussed, prestressing strands slip during transfer throughout the transfer length, tapering to zero at the end. Thus, a bond-slip relationship can be determined to represent the interaction between the strand and surrounding concrete. This study creates a bond-slip relationship based on the assumed bond stresses occurring in the plastic and elastic zones. Within the plastic zone the bond stress is constant; therefore, the bond-slip relationship is also constant. Likewise, within the elastic zone, the bond stress and the bond-slip relationship both taper to zero. Because the numerical modeling approach used in this study uses nonlinear springs to represent the bond-slip behavior, a force-versus-slip curve is needed rather than a bond-versus-slip curve. Each nonlinear spring is a bilinear curve (**Fig. 7**). The plateau of each curve is determined by multiplying the stress in the strand just after transfer (including losses due to elastic shortening) by its area to obtain the maximum force. The rate of force increase in the strand is then determined by dividing the maximum force by a specific transfer length, resulting in units of kip/in. (kN/mm), which is then multiplied by the desired nonlinear spring spacing converting the units back to kip (kN). Therefore, the force in the strand will increase at a constant rate for slip values between $0.025L_{es}$ and L_{es}.

An iterative process was used to determine the slip ($0.025L_{es}$) at the intersection between the ascending portion and the plateau of the nonlinear spring curves. Various percentages of slip were used in the models, and the strand force was plotted with respect to the distance from the end of the member (**Fig. 8**). In the transition zone around the transfer length (boxed region in Fig. 8), the rate of force increase in the strand varied with respect to the percentage of slip. Similar to the 95% average maximum strain method, to accurately model the application of prestress, at least 95% of the prestress force should be developed in the strand before reaching the specified transfer length. Therefore, of the four percentages evaluated, a slip equal to 2.5% of the total end slip consistently allows for the force in the strand to reach 95% of its maximum before the specified transfer length (**Fig. 9**).

Following are the steps used to generate the nonlinear spring curves for a 4 × 4 in. (100 × 100 mm) prism.

1. Identify the jacking stress f_{sj}, typically taken as $0.75f_{pu}$, where f_{pu} is the ultimate tensile strength of the strand.

2. Estimate loss of prestress due to relaxation *RET* (include shrinkage if not moist cured).

$$RET = f_{sj}\left(\frac{\log 24t - \log 24t_1}{45}\right)\left(\frac{f_{sj}}{f_{py}} - 0.55\right)$$

where

t = time at end of time step

t_1 = time at beginning of time step

f_{py} = specified yield strength of the strand

3. Calculate the stress in the strand just before transfer f_{si}.

4. Estimate loss of prestress due to elastic shortening *ES*.

$$ES = \left[\frac{\left(f_{si} - ES_{assumed}\right)A_{ps}}{A_g}\right]\left[\frac{E_{ps}}{E_{ci}}\right]$$

where

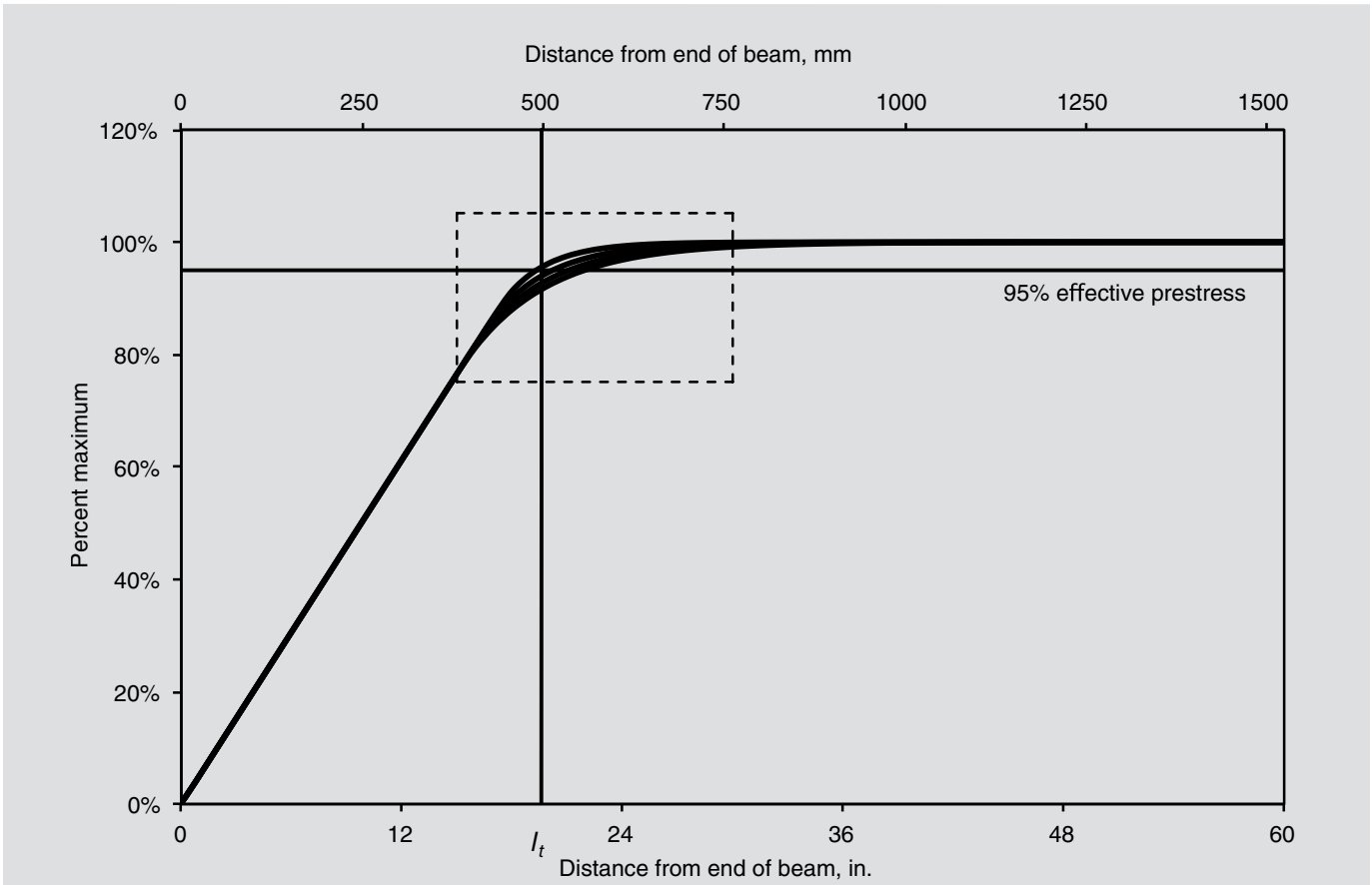

Figure 8. Nonlinear spring calibration curves. Note: l_t = transfer length.

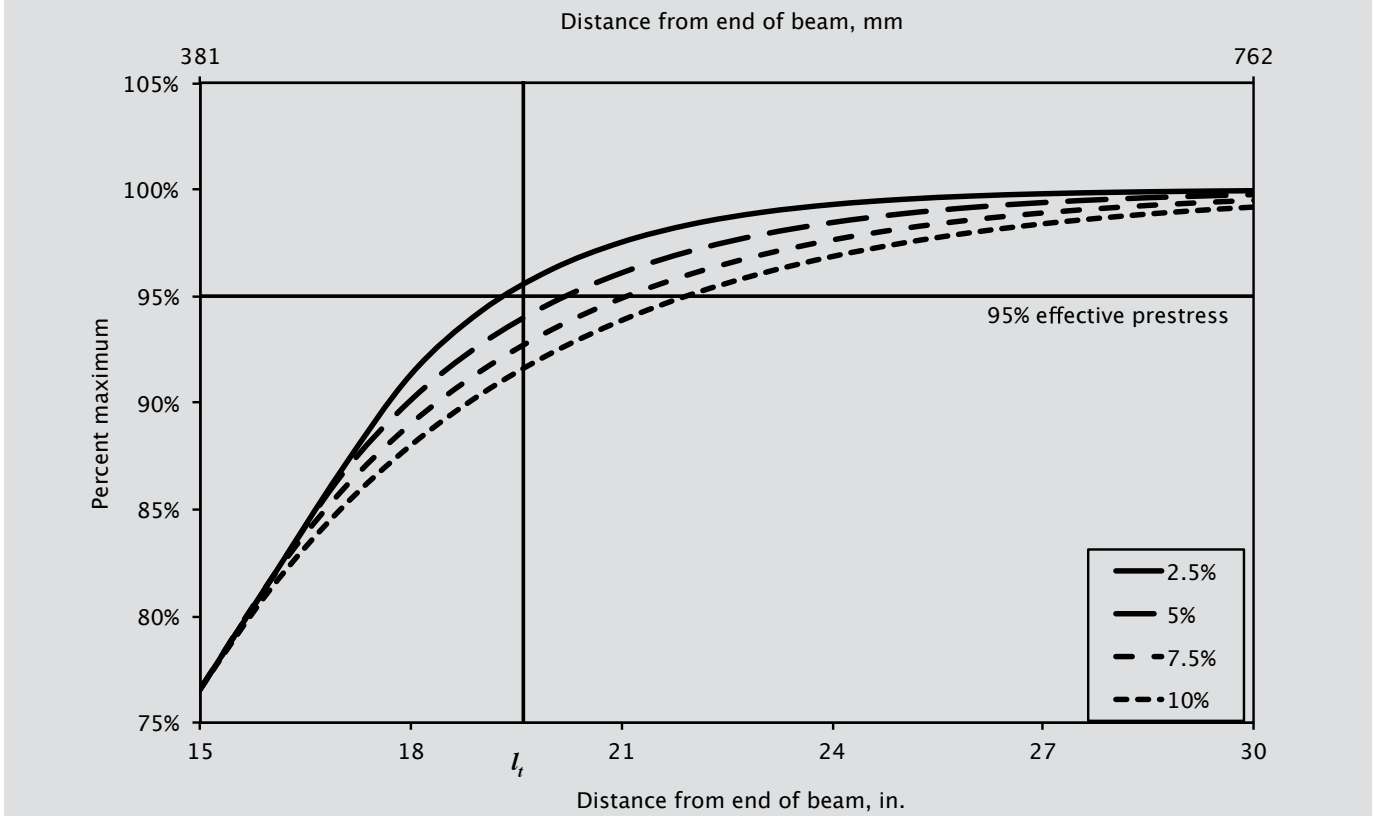

Figure 9. Detailed view of transition zone of nonlinear spring calibration curves. Note: l_t = transfer length.

Table 1. Numerical model verification summary

Model	Axial displacement, in.		Camber, in.		Strand force, kip		Maximum strain, 10^{-6}	
	Calculation	Analysis	Calculation	Analysis	Calculation	Analysis	Calculation	Analysis
Prism	0.0289	0.0300	n/a	n/a	28.4	28.4	492	493
Beam	0.0157	0.0164	0.0939	0.0936	29.4	29.4	264	264

Note: n/a = not applicable. 1 kip = 4.45 kN; 1 in. = 25.4 mm.

$ES_{assumed}$ = assumed loss of prestress due to elastic shortening

A_{ps} = area of prestressing strand

5. Calculate the stress in the strand just after transfer f_{so}.

6. Calculate the stress in the concrete at the elevation of the steel due to the prestress force only f_{cgs}.

7. Estimate end slip using specified transfer length using Eq. (8).

$$L_{es} = \frac{l_t}{2E_{ps}}\left(f_{so} + \frac{E_{ps}}{E_{ci}} f_{cgs}\right) \tag{8}$$

where

E_{ci} = modulus of elasticity of concrete at time of transfer

8. Develop a force-versus-displacement curve.

The prestress force is simulated by a change in temperature applied to the truss elements, resulting in an equivalent strain equal to that generated by the desired prestress force. While a temperature load is used, other programs may also allow for the use of an initial strain condition. In either case, the desired loading is based on the stress in the strand immediately before transfer, while losses due to elastic shortening are accounted for by deformation of the solid elements. Equations (9) and (10) are used to calculate the equivalent temperature load or strain, respectively. To further reduce computation time, symmetry was used at the midspan of each model and for the T beam models an additional plane of symmetry was used throughout their length.

$$\Delta T_{equiv} = \frac{f_{si}}{E_{ps}\alpha_{steel}} \tag{9}$$

where

ΔT_{equiv} = equivalent change in temperature in prestressing strand

α_{steel} = coefficient of thermal expansion for prestressing strand

$$\varepsilon_{equiv} = \frac{f_{si}}{E_{ps}} \tag{10}$$

where

e_{equiv} = equivalent strain in prestressing strand

Numerical model verification

Two models were created for verification before creating the full models and comparing with experimental data (**Table 1**). The first model was a 4 × 4 in. (100 × 100 mm) prism, 12 ft (3.7 m) long with a concentric prestress force. The second model was a 6 in. (150 mm) wide × 12 in. (300 mm) deep rectangular beam, 12 ft (3.7 m) long with an eccentric prestress force applied 4 in. below the neutral axis. The compressive strength of the concrete was assumed to be 4000 psi (287 MPa). The modulus of elasticity of the prestressing strands was assumed to be 28,500 ksi (196 GPa). Each model contained one $^1/_2$ in. (13 mm) diameter, 270 ksi (1860 MPa), low-relaxation prestressing strand, initially stressed to $0.75f_{pu}$ and having a transfer length of 25 in. (635 mm). For each model, a 7-day moist cure was assumed along with relaxation losses occurring over the same period, similar to the casting conditions of the test specimens included in this study. Furthermore, symmetry was used at the midspan of each model to reduce computation time.

Axial displacement, camber (beam only), strand force development, transfer lengths, and the maximum concrete surface strains were compared with calculated values. For the calculated values, the force in the strand was assumed to vary linearly from zero to the end of the specified transfer length and remain constant thereafter, including losses due to elastic shortening. Each displacement was calculated using virtual work. The longitudinal displacement due to application of prestress force δ_x for the prism and beam were calculated using Eq. (11) and (12), respectively, while the camber due to application of prestress force δ_y of the beam was calculated using Eq. (13). The transfer length was determined based on the distance from the end of the member for 95% of the force in the strand to be developed. Furthermore, the maximum strain was also calculated for each model. For initial comparisons, the self-weight was not taken into consideration, and the values in Table 1 only include the effects due to the application of prestress.

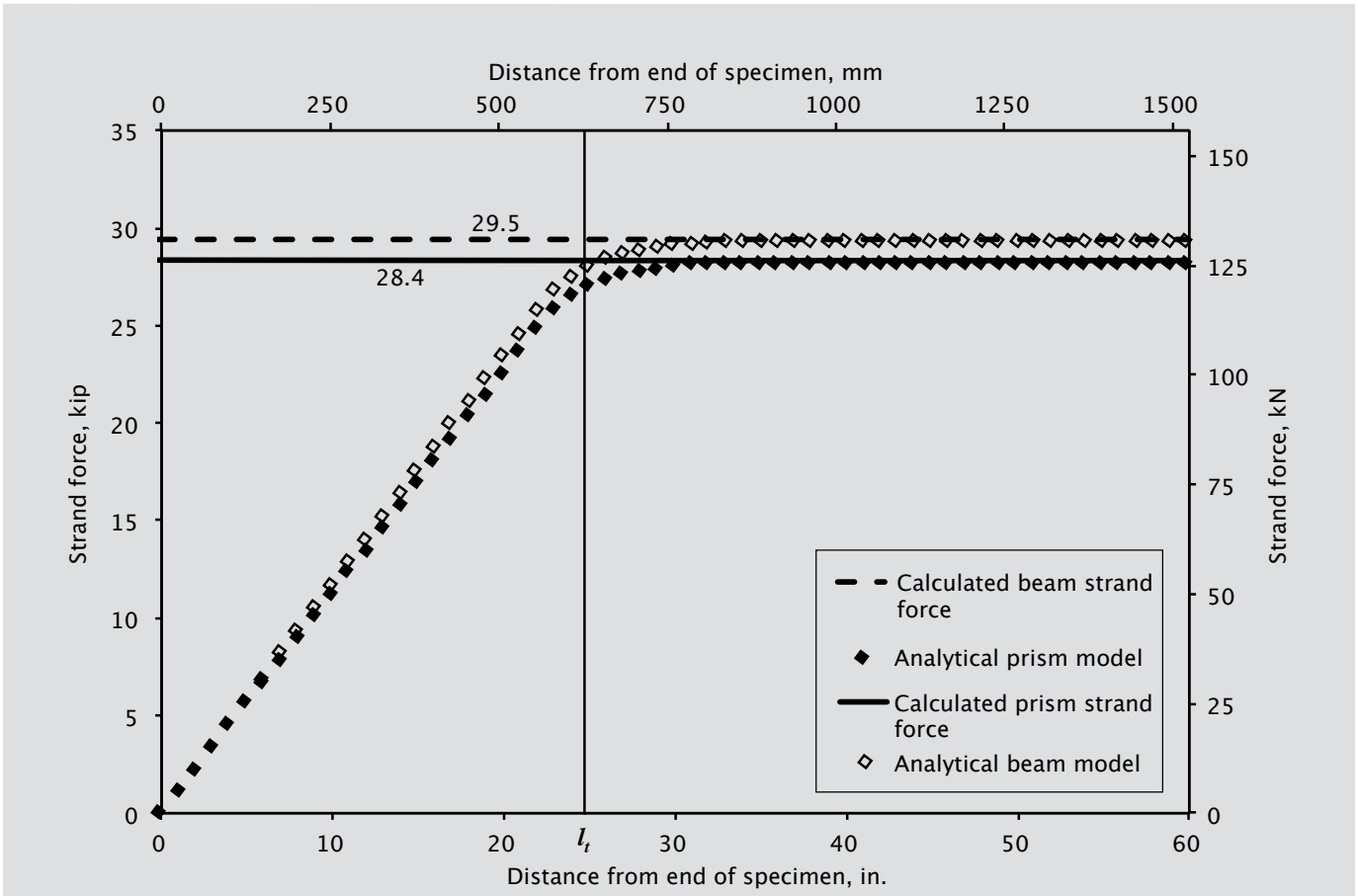

Figure 10. Strand force development in numerical trial models. Note: l_t = transfer length.

In addition, **Fig. 10** and **11** plot the strand force and the longitudinal surface strains at the elevation of the prestressing strand, respectively. Figure 10 includes the calculated theoretical force in the strand, including losses due to relaxation and elastic shortening, and the slight increase in strand force in the beam resulting from the self-weight. As expected, the force in the strand increased at a constant rate corresponding to the specified nonlinear spring force–versus–displacement curve, decreasing to zero as the strand force approached the calculated theoretical maximum. Furthermore, the force in the strands reached at least 95% of its maximum at or before a distance equal to the specified transfer length. Similar to Fig. 10, Fig. 11 also includes the calculated theoretical maximum strains, including the increase in strain in the beam due to the self-weight. The strain in the prism model increased as expected, with the rate gain decreasing to zero as the strain approached the calculated theoretical maximum. Likewise, the strain in the beam model also increased as expected, with the rate gain decreasing to zero as the strain approached the calculated theoretical maximum. However, the strain did slightly exceed the calculated theoretical maximum and then subsided, typical in strain profiles for beams. Also, like the force in the strand, the strain values reached at least 95% of maximum values at or before a distance equal to the specified transfer length.

$$\delta_x = \int_0^{l_t} \frac{P_o x}{l_t A_g E_{ci}} dx + \int_{l_t}^{L} \frac{P_o}{A_g E_{ci}} dx = \frac{P_o l_t}{2A_g E_{ci}} + \frac{P_o (L - l_t)}{A_g E_{ci}} \quad (11)$$

where

P_o = prestress force just after transfer

x = distance from each of member

A_g = gross cross-sectional area

L = length of numerical model

$$\delta_x = \int_0^{l_t} \frac{P_o x}{l_t A_g E_{ci}} + \frac{P_o x e^2}{l_t E_{ci} I_g} dx + \int_{l_t}^{L} \frac{P_o}{A_g E_{ci}} + \frac{P_o e^2}{E_{ci} I_g} dx$$
$$= \frac{P_o l_t}{2A_g E_{ci}} + \frac{P_o l_t e^2}{2E_{ci} I_g} + \frac{P_o (L - l_t)}{A_g E_{ci}} + \frac{P_o (L - l_t) e^2}{E_{ci} I_g} \quad (12)$$

where

e = strand eccentricity

I_g = gross moment of inertia

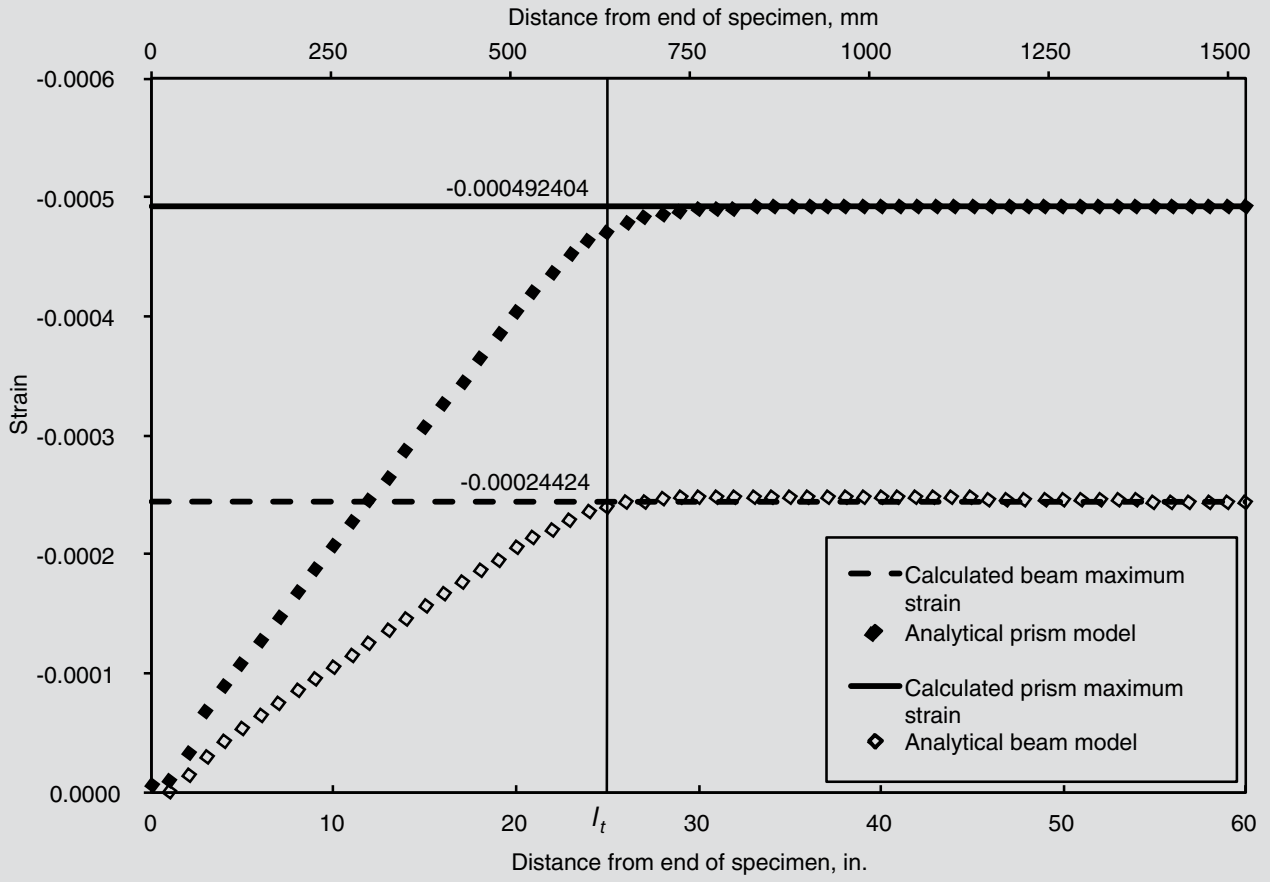

Figure 11. Concrete surface strain development in numerical trial models. Note: l_t = transfer length.

$$\delta_y = \int_0^{l_t} \frac{P_o e x^2}{l_t E_{ci} I_g} dx + \int_{l_t}^{L} \frac{P_o e x}{E_{ci} I_g} dx = \frac{P_o e l_t^2}{3E_{ci} I_g} + \frac{P_o e\left(L^2 - l_t^2\right)}{2E_{ci} I_g} \quad (13)$$

Comparison of analytical and experimental data

Twenty-three numerical models were compared with the experimental data acquired from various test specimens, including eight 4 × 4 in. (100 × 100 mm) prisms and 15 T beams. The nonlinear spring force–versus–displacement curve was developed for each model and was based on the measured transfer lengths and end-slip values calculated using Eq. (8). Each model also used the measured concrete compressive strength from the day of transfer and the material properties for the prestressing strands provided by the manufacturer. A nonlinear analysis was performed for each model, most of which proved sensitive to the convergence tolerance. **Figure 12** shows a typical T beam with camber and distribution of longitudinal stresses resulting from the applied prestress and self-weight using the modeling approach presented in this study. Also, **Table 2** shows a summary of the results from each of the numerical models, including comparisons for end slip, transfer length, and maximum concrete surface strains.

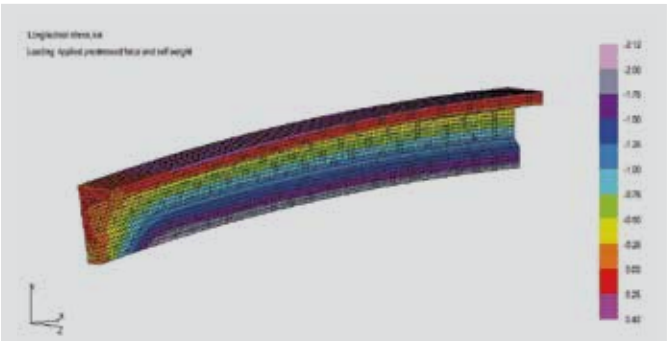

Figure 12. Sample contour plot showing longitudinal stress development in a typical T beam numerical model. Note: 1 ksi = 6.895 kPa.

The analytical end-slip values between the prestressing strands and surrounding concrete were calculated by the difference of the longitudinal displacements between the duplicate joints and their counterparts located at the ends of the test specimens. **Figure 13** compares the experimental end-slip values with the analytical end-slip values based on the numerical models. The data show a good correlation between calculated and experimental values, with a coefficient of determination R^2 of 0.84 and a slope of nearly 1 for the line of regression. Likewise, the transfer lengths were calculated based on the distance from the end

Table 2. Summary of results

Specimen	End slip, in.			Transfer length, in.			Maximum surface strain, 10^{-6}		
	Analysis	Experiment	Error, %	Analysis	Experiment	Error, %	Analysis	Experiment	Error, %
Prism 1	0.1056	0.1122	6.2	30.0	30.8	2.7	452	387	14.4
Prism 2	0.0820	0.0705	14.0	24.0	24.2	0.8	452	363	19.7
Prism 3	0.0656	0.0685	4.3	19.5	19.6	0.5	417	339	18.7
Prism 4	0.0539	0.0588	9.0	16.0	16.3	1.9	417	363	12.9
Prism 5	0.0735	0.0688	6.3	21.5	21.8	1.4	439	420	4.3
Prism 6	0.0828	0.0645	22.1	24.0	24.4	1.7	439	416	5.2
Prism 7	0.1056	0.1206	14.1	30.0	30.8	2.7	482	478	0.8
Prism 8	0.0865	0.0759	12.3	25.0	25.5	2.0	482	466	3.3
T beam 1	0.0360	0.0341	5.1	13.0	12.5	3.8	364	414	13.7
T beam 2	0.0391	0.0401	2.5	14.0	13.6	2.9	339	398	17.4
T beam 3	0.0452	0.0491	8.7	16.0	15.5	3.1	373	514	37.8
T beam 4	0.0407	0.0451	10.8	13.0	12.8	1.5	417	477	14.4
T beam 5	0.0548	0.0511	6.8	17.0	16.7	1.8	372	471	26.6
T beam 6	0.0431	0.0461	7.1	14.0	13.5	3.6	381	493	29.4
T beam 7	0.0453	0.0552	21.9	14.5	14.1	2.8	420	557	32.6
T beam 8	0.0497	0.0490	1.3	14.0	13.9	0.7	469	536	14.3
T beam 9	0.0747	0.0581	22.2	24.5	24.5	0.0	364	454	24.7
T beam 10	0.0591	0.0581	1.6	20.0	19.8	1.0	339	440	29.8
T beam 11	0.0662	0.0631	4.6	20.0	19.9	0.5	417	500	19.9
T beam 12	0.0587	0.0611	4.0	18.0	17.8	1.1	372	412	10.8
T beam 13	0.0797	0.0892	11.8	23.5	23.6	0.4	410	509	24.1
T beam 14	0.0702	0.0781	11.3	21.0	21.1	0.5	381	445	16.8
T beam 15	0.0708	0.0670	5.3	19.0	19.2	1.1	469	599	27.7
Average			9.3			1.7			18.2

Note: 1 in. = 25.4 mm.

of the member required for the force in the strand to reach 95% of the maximum. **Figure 14** compares the analytical and experimental transfer lengths. The data again showed an almost perfect correlation, with an R^2 of 1.00 and a slope of 1 for the line of regression. Such close correlation verifies the ability of the model to consistently produce the user-specified transfer lengths by simple modifications to nonlinear spring curves.

The force increase in the strand was also evaluated for each model. The force in the strand increased at a rate equal to the plateau of the nonlinear spring force–versus–displacement curve for each model and began to level off, approaching the calculated maximum around the transfer length. The maximum value of force developed in the strand for each model had a difference of less than 0.1% compared with the calculated force in the strand, including the losses due to elastic shortening. It was equally accurate when the self-weight was applied and the force in the strand slightly increased. To evaluate the force increase with respect to transfer length, the force in the strand for each model was normalized with respect to its maximum and plotted along with the normalized experimental concrete surface strains. **Figures 15** and **16** show typical comparative plots for a prism model and T beam model, respectively. Figure 15 shows the strand force and surface

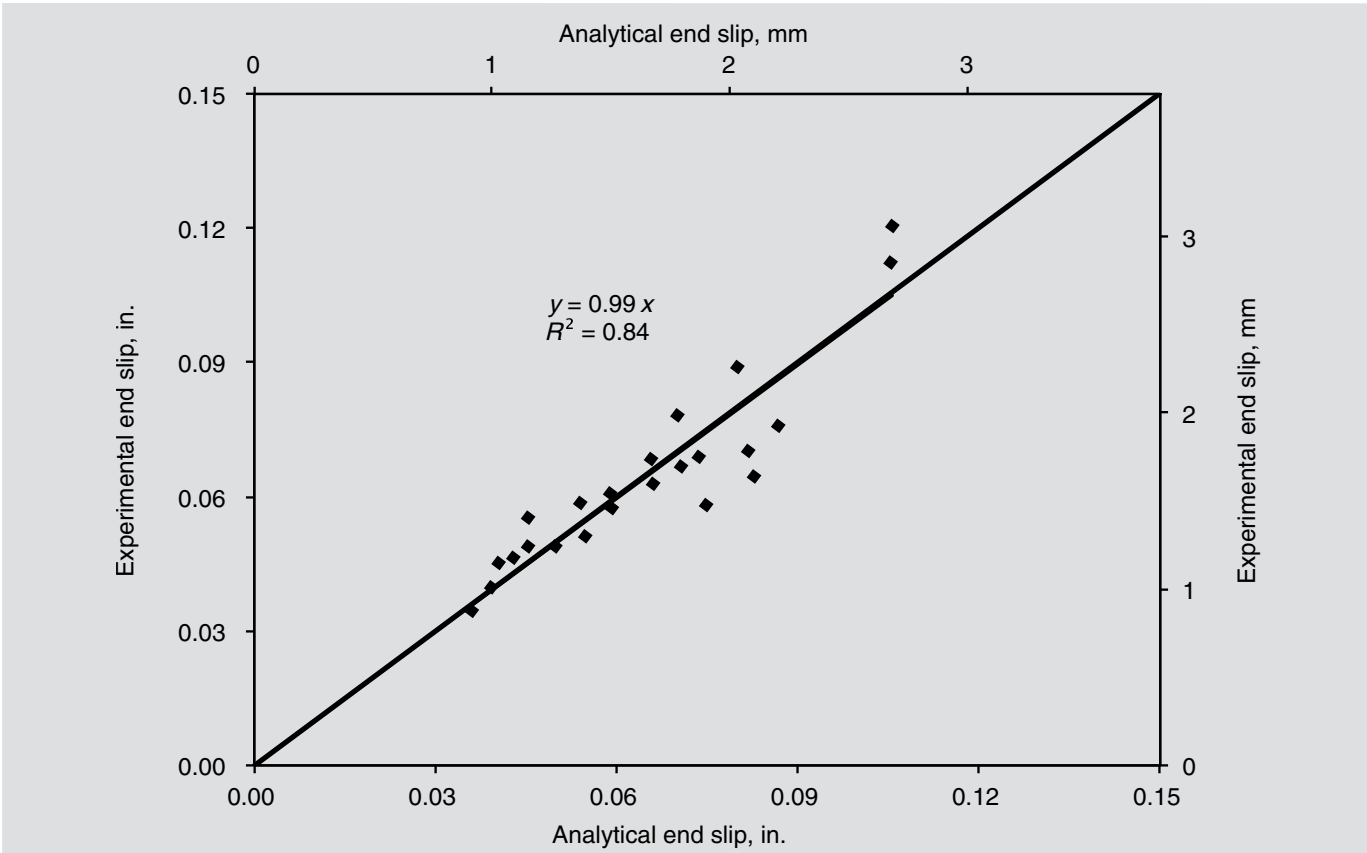

Figure 13. Correlation between experimental end-slip values and analytical end-slip values from numerical models.

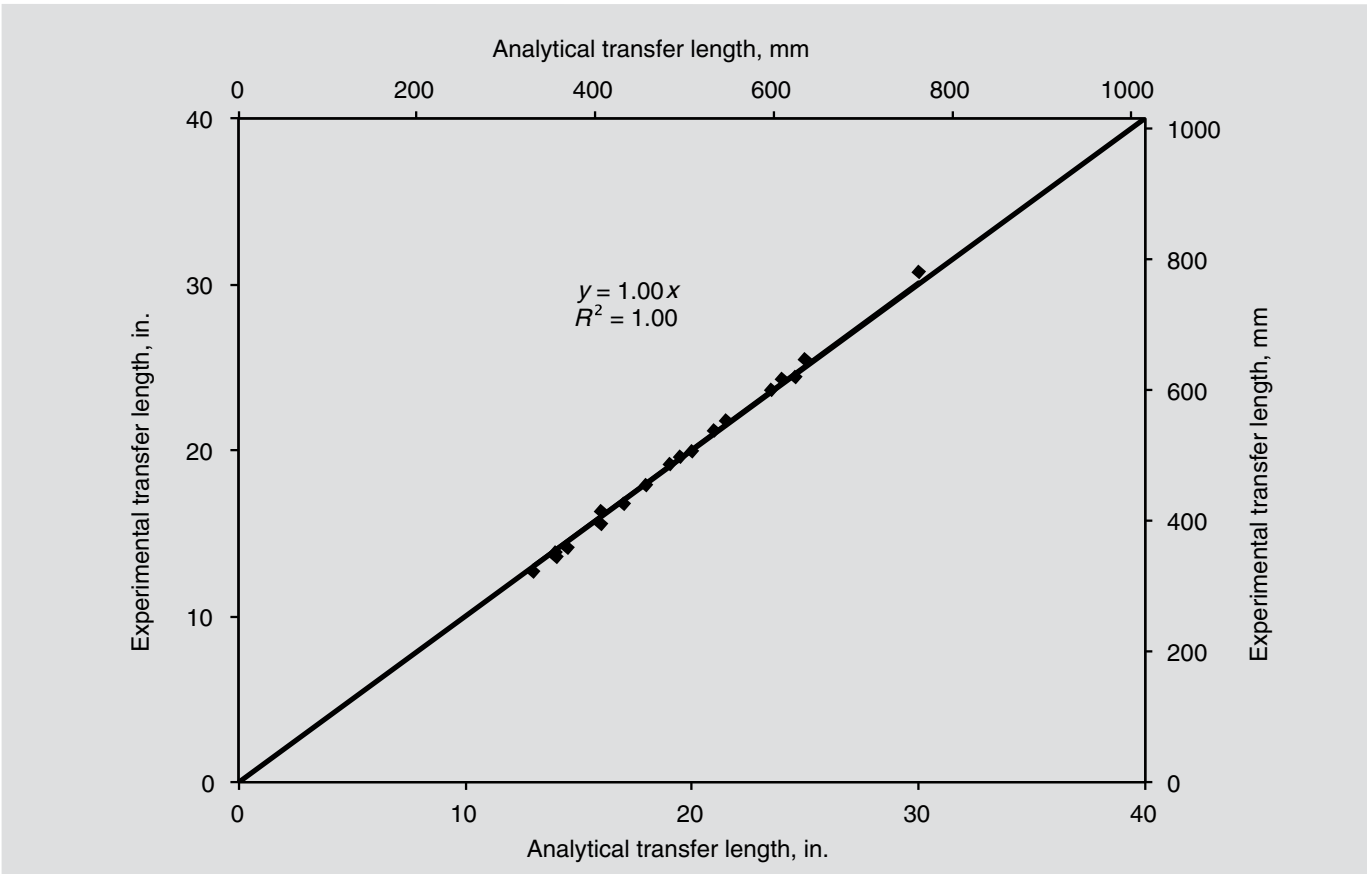

Figure 14. Correlation between transfer lengths from concrete surface strain measurements with analytical transfer length values from numerical models.
Note: R^2 = coefficient of determination.

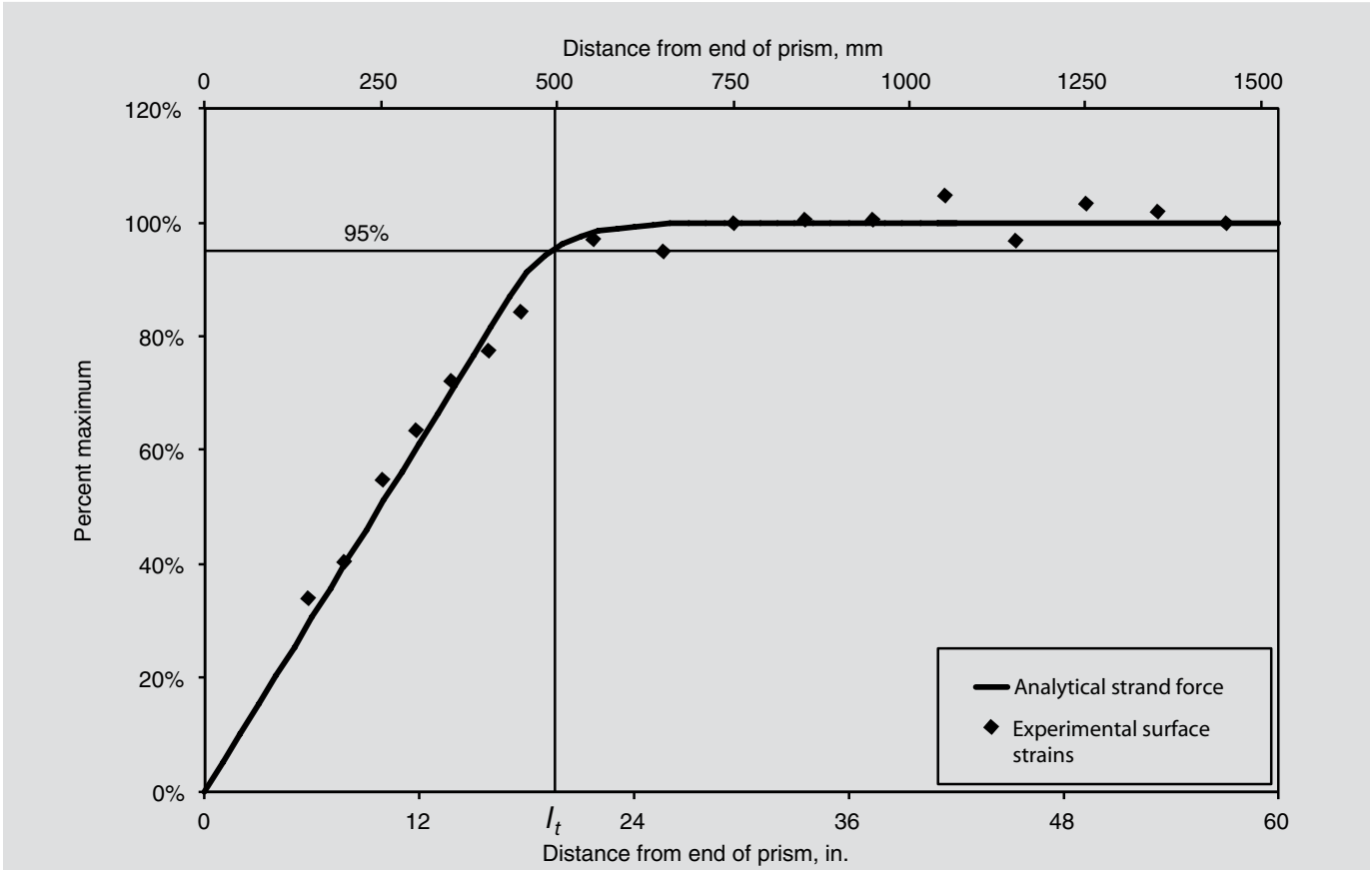

Figure 15. Comparison of normalized experimental concrete surface strains and analytical strand force for a typical prism model. Note: l_t = transfer length.

strains for a prism specimen to increase at the same relative rate and level off around the transfer length as expected. Likewise, Fig. 16 shows the strand force and surface strains for a T beam specimen to increase at the same relative rate and also level off around the transfer length. The only observable difference was the slight increase in concrete surface strains just beyond the transfer length, which is typical in prestressed concrete beams. Figures 15 and 16 also show the force in the strand to develop at least 95% of the maximum calculated value at a distance from the end of the member less than or equal to the specified transfer length.

Figure 17 compares the surface strains at the elevation of the strand with the experimental surface strains for a prism model. The analytical values increased within the transfer zone and began to level off near the transfer length, approaching the calculated maximum strain. While the experimental values also increased within the transfer zone and leveled off near the transfer length, the maximum strain was approximately 20% less than the calculated maximum strain. **Figure 18** compares the surface strains for a T beam model. In this case, the values again increased within the transfer zone and began to level off near the transfer length. However, the strains exceeded the calculated maximum before gradually decreasing to the calculated maximum, a typical trend in prestressed concrete beams. The experimental values also ascended above the average maximum and then descended but are still approximately 15% to 20% higher than the values obtained from the model. In both models the strain profiles were similar with variations between the maximums, which is likely due to variations in the concrete modulus of elasticity of the numerical models versus that of the experimental test specimens. The modulus of elasticity was estimated from the measured concrete strengths using the ACI 318-11 provisions.

Conclusion

A practical modeling approach is presented for finite element analysis of pretensioned, prestressed concrete members accounting for the transfer of prestress. The modeling approach uses existing knowledge of the relationship between transfer length and end slip, creating a force-versus-displacement curve representing the interface between the prestressing strand and surrounding concrete. The prestress force is simulated using equivalent temperature loads, and the materials are assumed to remain elastic. Twenty-three analytical models were constructed and compared with experimental data. The model accounts for bond-slip behavior and compares well with the experimental data for end slip, strand force development, transfer length, and concrete surface strains. The comparisons confirm the practicality and accuracy of the model.

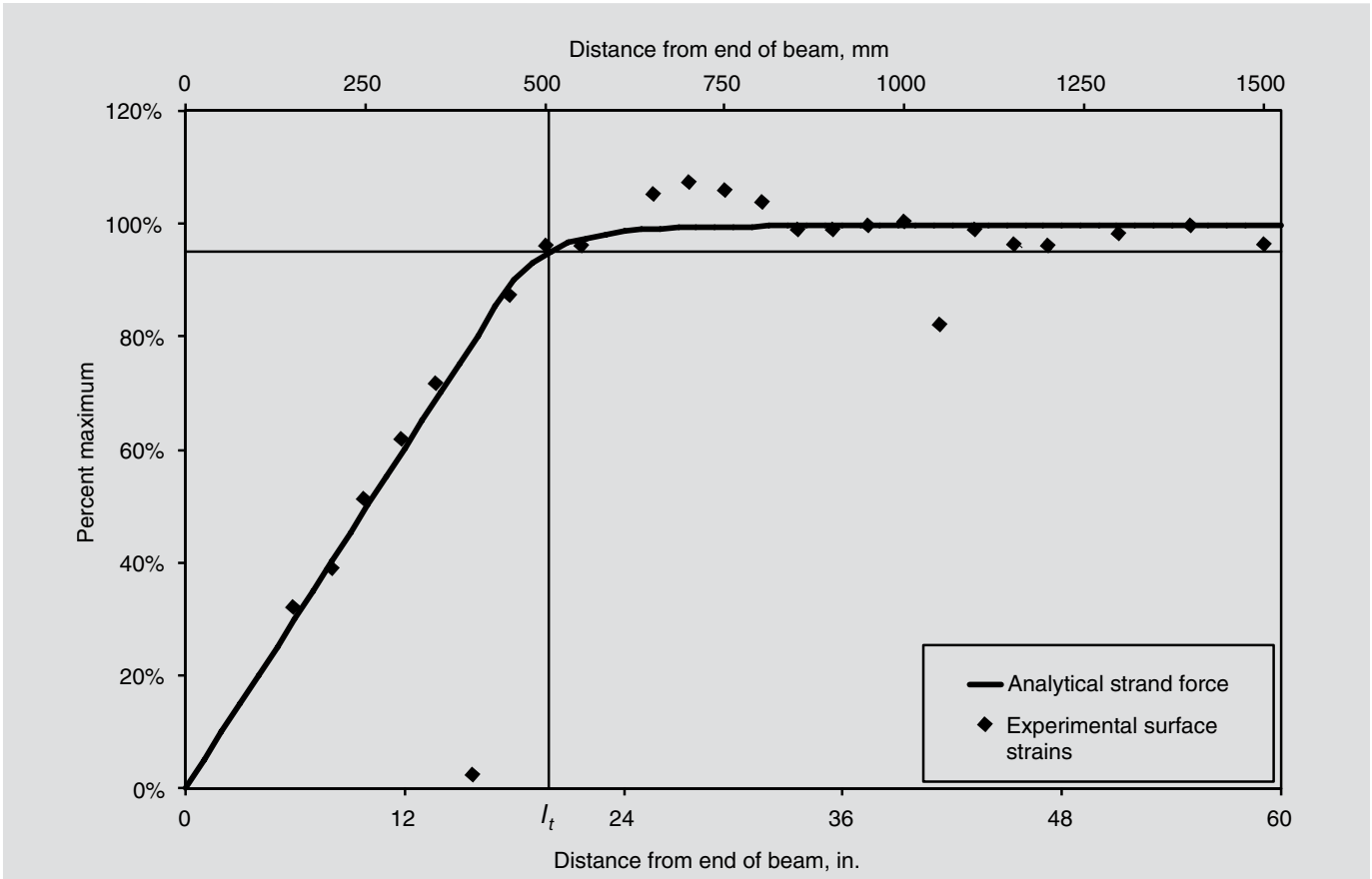

Figure 16. Comparison of normalized experimental concrete surface strains and analytical strand force for a typical T beam model. Note: l_t = transfer length.

Acknowledgments

The authors gratefully acknowledge the support provided by the Federal Highway Administration Innovative Bridge Research and Deployment Program and the Virginia Center for Transportation Innovation and Research. The authors express their gratitude to the technical staff of the Structural Engineering and Materials Laboratory at Virginia Polytechnic Institute and State University for their assistance in the preparation and testing of the specimens. The authors also express their thanks to Michael Swanger for his assistance during model development.

References

1. Janney, J. R. 1954. "Nature of Bond in Pre-Tensioned Prestressed Concrete." *ACI Journal* 50 (9): 717–736.

2. ACI (American Concrete Institute) Committee 318. 2011. *Building Code Requirements for Structural Concrete (ACI 318-11) and Commentary (ACI 318R-11)*. Farmington Hills, MI: ACI.

3. AASHTO (American Association of State Highway and Transportation Officials). 2010. *AASHTO LRFD Bridge Design Specifications*. Washington, DC: AASHTO.

4. Hanson, N. W., and P. H. Kaar. 1959. "Flexural Bond Tests of Pretensioned Prestressed Beams." *ACI Journal* 56 (1): 783–802.

5. Janney, J. R. 1963. "Report on Stress Transfer Length Studies on 270 ksi Prestressing Strand." *PCI Journal* 8 (1): 41–45.

6. Tabatabai, H., and T. J. Dickson. 1993. "The History of the Prestressing Strand Development Length Equation." *PCI Journal* 38 (6): 64–75.

7. ACI Committee 318. 1963. *Building Code Requirements for Structural Concrete (ACI 318-63) and Commentary (ACI 318-63)*. Farmington Hills, MI: ACI.

8. Buckner, C. D. 1995. "A Review of Strand Development Length for Pretensioned Concrete Members." *PCI Journal* 40 (2): 84–105.

9. Martin, A. R., and N. L. Scott. 1976. "Development of Prestressing Strand in Pretensioned Member." *ACI Journal* 73 (8): 453–456.

10. Zia, P., and T. Mostafa. 1977. "Development Length of Prestressing Strands." *PCI Journal* 22 (5): 54–63.

11. Cousins, T. E., D. W. Johnston, and P. Zia. 1990.

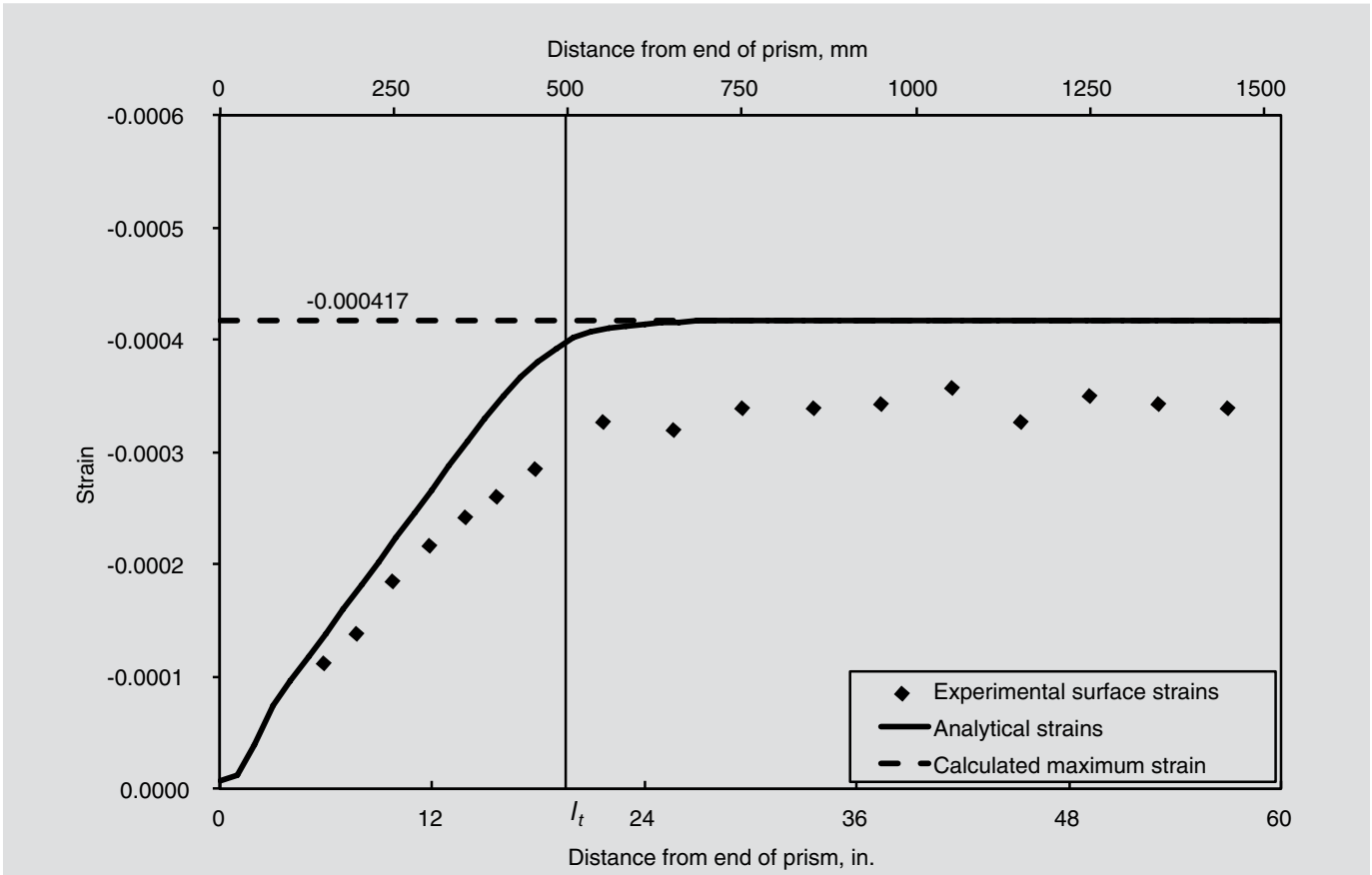

Figure 17. Comparison of experimental concrete surface strains and analytical concrete surface strains for a typical prism model. Note: l_t = transfer length.

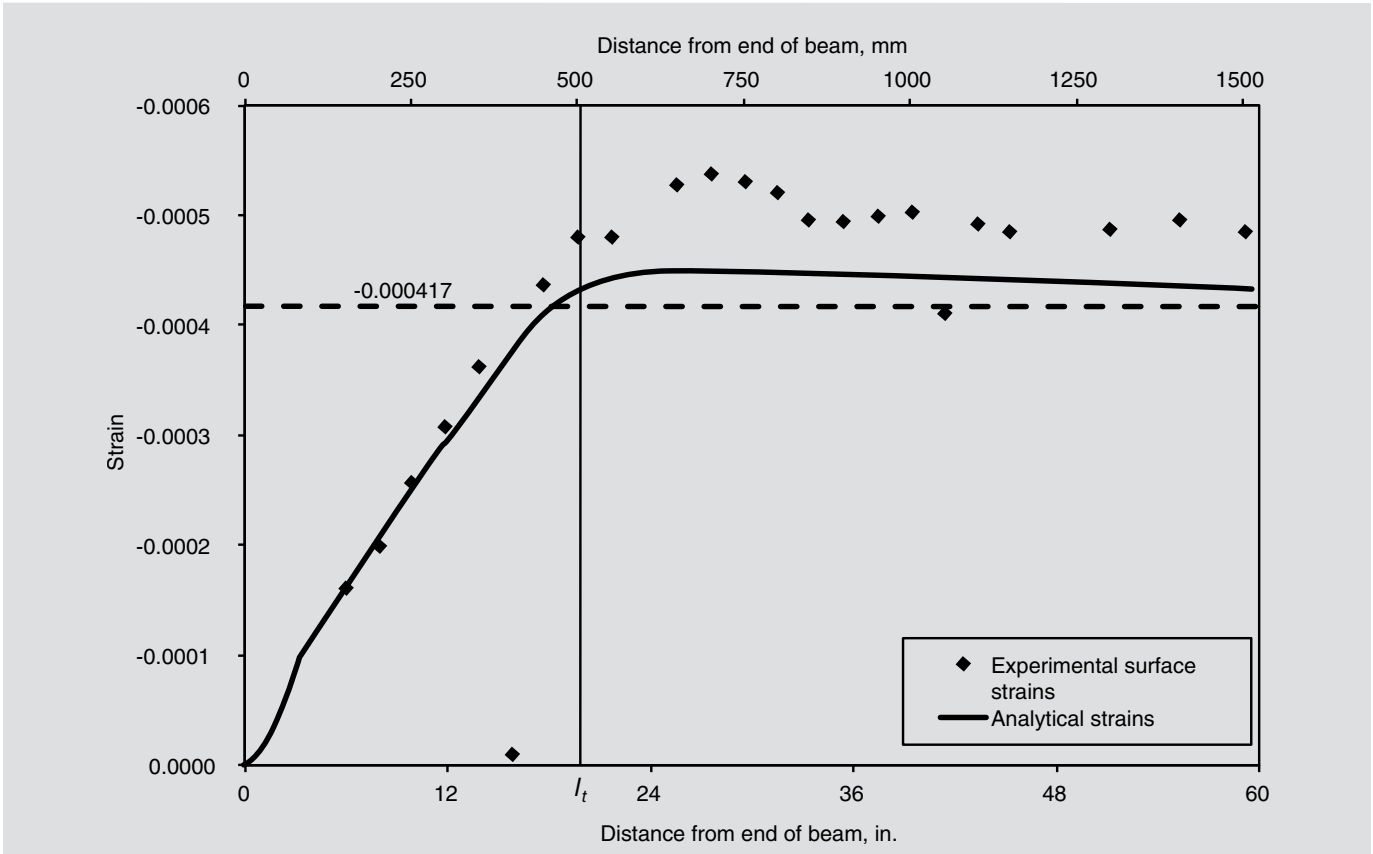

Figure 18. Comparison of experimental concrete surface strains and analytical concrete surface strains for a typical T beam model. Note: l_t = transfer length.

"Transfer and Development of Epoxy Coated and Uncoated Prestressing Strand." *PCI Journal* 35 (4): 92–103.

12. Shahawy, M. A., M. Issa, and B. D. Batchelor. 1992. "Strand Transfer Length in Full Scale AASHTO Prestressed Concrete Girders." *PCI Journal* 37 (3): 84–96.

13. Mitchell, D., W. D. Cook, A. A. Khan, and T. Tham. 1993. "Influence of High Strength Concrete on Transfer and Development Length of Prestressing Strand." *PCI Journal* 38 (3): 52–66.

14. Deatharage, J. H., E. G. Burdette, and C. K. Chew. 1994. "Development Length and Lateral Spacing Requirements of Prestressing Strand for Prestressed Concrete Bridge Girders." *PCI Journal* 39 (1): 70–83.

15. Russell, B. W., and N. H. Burns. 1997. "Measurement of Transfer Lengths on Pretensioned Concrete Elements." *Journal of Structural Engineering* 123 (5): 541–549.

16. Lane, S. H. 1998. *A New Development Length Equation for Pretensioned Strands in Bridge Beams and Piles*. McLean, VA: Federal Highway Administration Structures Division.

17. Barnes, R. W., J. W. Grove, and N. H. Burns. 2003. "Experimental Assessment of Factors Affecting Transfer Length." *ACI Structural Journal* 100 (6): 740–748.

18. Kose, M. M., and W. R. Burkett. 2005. "Formulation of New Development Length Equation for 0.6 in. Prestressing Strand." *PCI Journal* 50 (5): 96–105.

19. Peterman, R. J. 2007. "The Effects of As-Cast Depth and Concrete Fluidity on Strand Bond." *PCI Journal* 52 (3): 72–101.

20. Ramírez, J. A., and B. W. Russell. 2008. *Transfer, Development, and Splice Length for Strand/Reinforcement in High-Strength Concrete*. Report 603. Washington, D.C.: National Cooperative Highway Research Project.

21. Martí-Vargas, J. R., P. Serna, J. Navarro-Gregori, and J. L. Bonet. 2012. "Effects of Concrete Composition on Transmission Length of Prestressing Strands." *Construction and Building Materials* 27 (1): 350-356.

22. Martí-Vargas, J. R., P. Serna, J. Navarro-Gregori, and L. Pallares. 2012. "Bond of 13 mm Prestressing Steel Strands in Pretensioned Concrete Members." *Engineering Structures* 41: 403–412.

23. Cousins, T. E., D. W. Johnston, and P. Zia. 1990. "Transfer Length of Epoxy-Coated Prestressing Strand." *ACI Materials Journal* 87 (3): 193–203.

24. Guyon, Y. 1960. *Prestressed Concrete*. Vol. 1. New York, NY: John Wiley and Sons Inc.

25. Martí-Vargas, J. R., C. A. Arbeláez, P. Serna-Ros, and C. Castro-Bugallo. 2007. "Reliability of Transfer Length Estimation from End Slip." *ACI Structural Journal* 104 (4): 487–494.

26. Balazs, G. L. 1993. "Transfer Length of Prestressing Strand as a Function of Draw-In and Initial Prestress." *PCI Journal* 38 (2): 86–93.

27. Kose, M. M. 2007. "Prediction of Transfer Length of Prestressing Strands Using Neural Networks." *ACI Structural Journal* 104 (2): 162–169.

28. Kose, M. M. and Kayadelen, C. 2010. "Modeling of Transfer Length of Prestressing Strands Using Genetic Programming and Neuro-Fuzzy." *Advanced Engineering Software* 41 (2): 315-322.

29. Martí-Vargas, J. R., F. J. Ferri, and V. Yepes. 2013. "Prediction of the Transfer Length of Prestressing Strands with Neural Networks." *Computers and Concrete* 12 (2): 187-209.

30. Aalami, B. O. 1990. "Load Balancing—A Comprehensive Solution to Post-tensioning." *ACI Structural Journal* 87 (6): 662–670.

31. Kannel, J., C. French, and H. Stolarski. 1997. "Release Methodology of Strands to Reduce End Cracking in Pretensioned Concrete Girders." *PCI Journal* 42 (1): 42–54.

32. Ayoub, A., and F. C. Filippou. 2010. "Finite-Element Model for Pretensioned Prestressed Concrete Girders." *Journal of Structural Engineering* 136 (4): 401–409.

33. Arab, A. A., S. S. Badie, and M. T. Manzari. 2011. "A Methodological Approach for Finite Element Modeling of Pretensioned Concrete Members at the Release of Pretensioning." *Engineering Structures* 33 (6): 1918–1929.

34. Eligehausen, R., E. P. Popov, and V. V. Bertero. 1983. "Local Bond Stress-Slip Relationships of Deformed Bars under Generalized Excitations." Berkeley, CA: University of California Earthquake Engineering Research Center.

35. Russell, B. W., and N. H. Burns. 1993. *Design Guidelines for Transfer, Development and Debonding of Large Diameter Seven Wire Strands in Pretensioned*

Concrete Girders. Research report 1210-5F. Austin, TX: The University of Texas at Austin Center for Transportation Research.

Notation

A_g = gross cross-sectional area

A_{ps} = area of prestressing strand

b = power of bond stress relationship

d_b = strand diameter

e = strand eccentricity

E_{ci} = modulus of elasticity of concrete at transfer

E_{ps} = modulus of elasticity of prestressing strands

ES = loss of prestress due to elastic shortening

$ES_{assumed}$ = assumed loss of prestress due to elastic shortening

f'_{ci} = concrete compressive strength at transfer

f_{cgs} = stress in concrete at elevation of strands due to prestress

f_{pu} = ultimate tensile strength of strand

f_{py} = specified yield strength of strand

f_{se} = effective prestress in strand after all losses

f_{si} = stress in strand just before transfer

f_{sj} = jacking stress

f_{so} = stress in strand just after transfer

I_g = gross moment of inertia

l_t = transfer length

L = length of numerical model

L_{es} = end slip

P_o = prestress force just after transfer

R^2 = coefficient of determination

RET = loss of prestress due to relaxation

s = nonlinear spring spacing

t = time at end of time step

t_1 = time at beginning of time step

U_t = plastic transfer bond stress

x = distance from end of member

α = bond stress distribution factor

α_{steel} = coefficient of thermal expansion for prestressing strand

δ_c = elastic shortening of concrete within transfer zone

δ_s = sum of elastic shortening and end slip

δ_x = longitudinal displacement due to application of prestress force

δ_y = camber due to application of prestress force

ΔT_{equiv} = equivalent change in temperature in prestressing strand

$\varepsilon_c(x)$ = strain in concrete along transfer length

ε_{co} = strain in concrete just after transfer

ε_{equiv} = equivalent strain in prestressing strand

$\varepsilon_s(x)$ = strain in strand along transfer length

ε_{si} = strain in strand just before transfer

ε_{so} = strain in strand just after transfer

Nonlinear spring force–versus–displacement curve and equivalent load calculation example

Given:

4 × 4 in. (100 × 100 mm) concrete prism

Concrete compressive strength at transfer f'_{ci} = 5700 psi (39.3 MPa)

$E_{ci} = 57\sqrt{f'_{ci}} = 57\sqrt{5700}$ = 4303 ksi (29.67 MPa)

E_{ps} = 28,500 ksi (196,500 MPa)

α_{steel} = 6.5 × 10-6 in./in./°F (1.17 × 10-5 mm/mm/°C)

A_g = 16 in.^{2} (10,300 mm^2)

A_{ps} = 0.153 in.^{2} (98.7 mm^2)

l_t = 19.59 in. (497.6 mm)

$ES_{assumed}$ = 11.89 ksi

nonlinear spring spacing s = 1 in. (25.4 mm)

1. Identify jacking stress f_{sj}, typically taken as $0.75f_{pu}$

   $f_{sj} = (0.75)(270) = 202.5$ ksi (1396 MPa)

2. Estimate loss of prestress due to relaxation (include shrinkage if not moist cured)

$$RET = f_{sj}\left(\frac{\log 24t - \log 24t_1}{45}\right)\left(\frac{f_{sj}}{f_{py}} - 0.55\right)$$

$$= 202.5\left[\frac{\log 24(7) - \log 24(1/24)}{45}\right]\left(\frac{202.5}{243} - 0.55\right)$$

   = 2.84 ksi (20 MPa)

3. Calculate stress in strand just before transfer f_{si}

   $f_{si} = 202.5 - 2.84 = 199.66$ ksi (1377 MPa))

4. Estimate loss of prestress due to elastic shortening

$$ES = \left[\frac{(f_{si} - ES_{assumed})A_{ps}}{A_g}\right]\left[\frac{E_{ps}}{E_{ci}}\right]$$

$$= \left[\frac{(199.66 - 11.89)(0.153)}{16}\right]\left[\frac{28,500}{4303}\right]$$

   = 11.89 ksi (81.98 MPa)

5. Calculate stress in strand just after transfer f_{so}

   $f_{so} = 199.66 - 11.89 = 187.77$ ksi (1295 MPa)

6. Calculate stress in concrete at elevation of steel due to prestress force only f_{cgs}

$$f_{cgs} = \frac{f_{so}A_{ps}}{A_g} = \frac{(187.77)(0.153)}{16}$$

   = 1.80 ksi (12.4 MPa)

7. Estimate end slip using transfer length

$$L_{es} = \frac{l_t}{2E_{ps}}\left(f_{so} + \frac{E_{ps}}{E_{ci}}f_{cgs}\right)$$

$$= \frac{19.59}{(2)(28,500)}\left[187.77 + \left(\frac{28,500}{4303}\right)(1.80)\right]$$

   = 0.068631 in. (1.743 mm)

8. Develop force-versus-displacement curve

$$\frac{f_{so}A_{ps}s}{l_t} = \frac{(188.77)(0.153)(1)}{19.59}$$

   = 1.467 kip (6.525 kN)

   $(2.5\%)L_{es} = (0.025)(0.068631) = 0.001716$ in. (0.04358 mm)

Finally, calculate equivalent temperature load and equivalent strain.

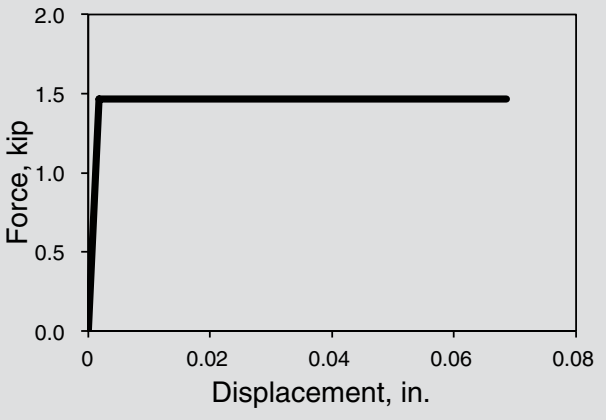

$$\Delta T_{equiv} = \frac{f_{si}}{E_{ps}\alpha_{steel}} = \frac{199.66}{(28{,}500)\left(6.5\times10^{-6}\right)}$$

$$= 1078°\text{F } (581°\text{C})$$

$$\varepsilon_{equiv} = \frac{f_{si}}{E_{ps}} = \frac{199.66}{28{,}500} = 0.007006$$

About the authors

J. Chris Carroll, PhD, is an assistant professor in the Department of Civil Engineering at the University of Louisiana at Lafayette.

Thomas E. Cousins, PhD, PE, is a professor in the Department of Civil and Environmental Engineering at Virginia Polytechnic Institute and State University in Blacksburg, Va.

Carin L. Roberts-Wollmann, PhD, PE, is a professor in the Department of Civil and Environmental Engineering at Virginia Polytechnic Institute and State University.

Abstract

This paper presents a numerical modeling approach that accounts for slip between prestressing strands and the surrounding concrete within the transfer zone. The objective of the study was to develop a modeling approach that can accurately and efficiently predict member behavior based on specified transfer lengths. The modeling approach uses three components: a matrix of solid elements to represent the concrete, truss elements to represent the prestressing strand, and nonlinear springs accounting for the interface between the prestressing strand and surrounding concrete. The force-versus-displacement curves for the nonlinear springs are based on the known relationship between end slip and transfer length. The results of 23 numerical models are included and compared with experimental data from corresponding test specimens. The study confirms the practicality and accuracy of the modeling approach to predict member behavior based on specified transfer lengths.

Keywords

Bond-slip behavior, bond stress, end slip, end-zone behavior, finite element modeling, nonlinear springs, transfer length.

Review policy

This paper was reviewed in accordance with the Precast/Prestressed Concrete Institute's peer-review process.

Reader comments

Please address and reader comments to journal@pci.org or Precast/Prestressed Concrete Institute, c/o *PCI Journal*, 200 W. Adams St., Suite 2100, Chicago, IL 60606.